Reaction of 6-Methyl-2,2′-bipyridine with 1,2-$Os_3(CO)_{10}(MeCN)_2$: Syntheses, Reductive Elimination/Ligand Displacement Kinetics, and X-ray Diffraction Structures of the Isomeric Clusters $HOs_3(CO)_9(\mu_2\text{-}N_2C_{11}H_9)$ and $H_2Os_3(CO)_8(\mu_3\text{-}N_2C_{11}H_8)$

Bhaskar Poola,[†] Carl J. Carrano,[‡] and Michael G. Richmond*,[†]

Department of Chemistry, University of North Texas, Denton, Texas 76203-5070, and Department of Chemistry and Biochemistry, San Diego State University, San Diego, California 82182-1030

Received January 8, 2008

Treatment of $Os_3(CO)_{10}(MeCN)_2$ (**1**) with the heterocyclic ligand 6-methyl-2,2′-bipyridine (6-Me-2,2′-bpy) at room temperature leads to the formation of the isomeric hydride-bridged clusters $HOs_3(CO)_9(\mu_2\text{-}CH_2N_2C_{10}H_7)$ (**2**) and $HOs_3(CO)_9(\mu_2\text{-}N_2C_{11}H_9)$ (**3**). The cyclometalation of the ancillary 6-Me group in **2** and the *ortho* metalation of the nonsubstituted pyridyl ring in **3** have been confirmed by spectroscopic and crystallographic methods. Thermolysis of **2** leads to the formation of **3** and the dihydride cluster $H_2Os_3(CO)_8(\mu_3\text{-}N_2C_{11}H_8)$ (**4**); the latter cluster, whose structure has been crystallographically determined, derives from a formal loss of CO and C−H bond activation of the methylene moiety in **2**. Heating **2** in the presence of ligand-trapping agents proceeds with the release of the 6-Me-2,2′-bpy ligand and formation of $Os_3(CO)_9L_3$ [where L = CO, $P(OMe)_3$]. The kinetics for the reaction between **2** and added ligand have been investigated by UV−vis and NMR spectroscopies and found to be first-order in starting cluster and independent of the incoming ligand. Parallel kinetic experiments employing the deuterated cluster $DOs_3(CO)_9(\mu_2\text{-}CD_2N_2C_{10}H_7)$ (**2**-d_3), which was prepared from cluster **1** and 6-Me-d_3-2,2′-bpy, confirm the existence of a primary kinetic isotope effect (KIE) of 1.78 at 323 K. The KIE data and the calculated activation parameters [$\Delta H^{\ddagger} = 21.7(4)$ kcal/mol; $\Delta S^{\ddagger} = -13(1)$ eu] are strongly suggestive of a reaction scheme involving a rate-limiting reductive coupling of the bridging hydride ligand and cyclometalated alkyl moiety in **2** to furnish a putative sigma complex containing an intact methyl group bound to the Os_3 cluster, prior to the generation of the unsaturated cluster $Os_3(CO)_9(\mu\text{-}N_2C_{11}H_{10})$. Thermolysis of **3** in the presence of added $P(OMe)_3$ does not furnish free 6-Me-2,2′-bpy but proceeds by a ligand-induced displacement of the methyl-substituted pyridyl ring and formation of the cluster compound $HOs_3(CO)_9[P(OMe)_3](\mu_2\text{-}N_2C_{11}H_9)$ (**5**). The kinetics for the reaction between **3** and $P(OMe)_3$ have been studied over the temperature range 333−356 K, and on the basis of the observed activation parameters [$\Delta H^{\ddagger} = 13.0(3)$ kcal/mol; $\Delta S^{\ddagger} = -30(1)$ eu] and the first-order dependence on the cluster and ligand, an associative process that involves $P(OMe)_3$ ligand attack on the cluster and release of the methyl-substituted pyridyl ring in the rate-limiting step is proposed.

Introduction

The catalytic activation of C−H bonds in nitrogen-containing heterocyles continues to captivate the attention and research efforts of many academic and industrial groups.[1] Here the efficient production of commodity pharmaceutical chemicals via alternative methodologies provides the continuing allure and incentive for practitioners wishing to demonstrate selective protocols for the functionalization of C−H bonds in heterocyclic substrates. Some of these transformations that have achieved distinction include the coupling of N-heterocycles with alkenes and arenes, site-specific carbonylations, and nucleophilic addition reactions to metal-activated heterocyclic platforms.[2] Representative paradigms of these reactions are shown in eqs 1−3.

Recent reports from Cabeza and co-workers have demonstrated the facile activation of the C−H bonds in an ancillary methyl group in 6,6′-Me_2-2,2′-bipyridine and 2,9-Me_2-1,10-phenanthroline by $Ru_3(CO)_{12}$ to furnish the corresponding cyclometalated clusters $H_2Ru_3(CO)_8(\mu_3\text{-HCN-NMe})$ (where N-N = 2,2′-bpy, 1,10-phen).[3] Thermolysis of these products in the presence of added $Ru_3(CO)_{12}$ affords the *ortho*-metalated carbide clusters $HRu_5(\mu_5\text{-C})(CO)_{13}(\mu\text{-N-NMe})$ through a chelate-assisted bond activation sequence, with eq 4 illustrating these ligand

* Corresponding author. E-mail: cobalt@unt.edu.
[†] University of North Texas.
[‡] San Diego State University.

(1) (a) Ritleng, V.; Sirlin, C.; Pfeffer, M. *Chem. Rev.* **2002**, *102*, 1731. (b) Pastine, S. J.; Youn, S. W.; Sames, D. *Tetrahedron* **2003**, *59*, 8859. (c) Zificsak, C. A.; Hlasta, D. J. *Tetrahedron* **2004**, *60*, 8991. (d) Tobisu, M.; Chatani, N. *Angew. Chem., Int. Ed.* **2006**, *45*, 1683. (e) Godula, K.; Sames, D. *Science* **2006**, *312*, 67. (f) Campos, K. R. *Chem. Soc. Rev.* **2007**, *36*, 1069.

(2) (a) Bergman, B.; Holmquist, R.; Smith, R.; Rosenberg, E.; Ciurash, J.; Hardcastle, K.; Visi, M. *J. Am. Chem. Soc.* **1998**, *120*, 12818. (b) Smith, R.; Rosenberg, E.; Hardcastle, K. I.; Vazquez, V.; Roh, J. *Organometallics* **1999**, *18*, 3519. (c) Chatani, N.; Asaumi, T.; Ikeda, T.; Yorimitsu, S.; Ishii, Y.; Kakiuchi, F.; Murai, S. *J. Am. Chem. Soc.* **2000**, *122*, 12882. (d) Chatani, N.; Asumi, T.; Yorimitsu, S.; Ikeda, T.; Kakiuchi, F.; Murai, S. *J. Am. Chem. Soc.* **2001**, *123*, 10935. (e) Rosenberg, E.; Kabir, S. E.; Abedin, M. J.; Hardcastle, K. I. *Organometallics* **2004**, *23*, 3982. (f) Wiedemann, S. H.; Lewis, J. C.; Ellman, J. A.; Bergman, R. G. *J. Am. Chem. Soc.* **2006**, *128*, 2452. (g) Wiedemann, S. H.; Ellman, J. A.; Bergman, R. G. *J. Org. Chem.* **2006**, *71*, 1969. (h) Lewis, J. C.; Wu, J. Y.; Bergman, R. G.; Ellman, J. A. *Angew. Chem., Int. Ed.* **2006**, *45*, 1589. (i) Lewis, J. C.; Bergman, R. G.; Ellman, J. A. *J. Am. Chem. Soc.* **2007**, *129*, 5332. (j) Musaev, D. G.; Nowroozi-Isfahani, T.; Morokuma, K.; Abedin, J.; Rosenberg, E.; Hardcastle, K. I. *Organometallics* **2006**, *25*, 203.

10.1021/om800020x CCC: $40.75
Publication on Web 06/07/2008

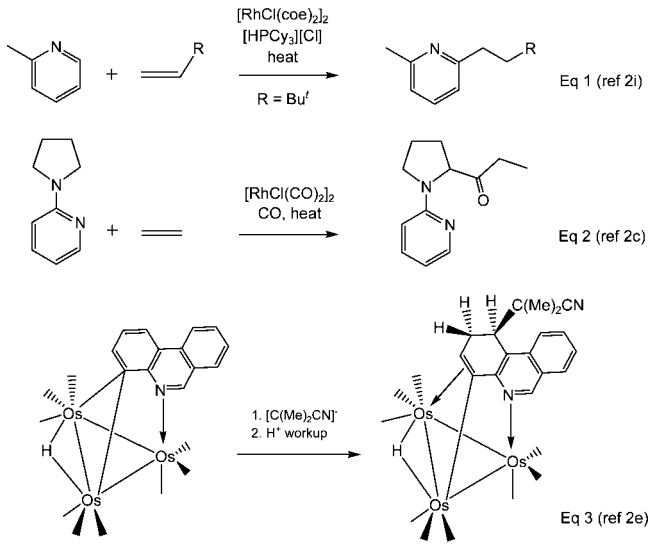

activation sequences using the 6,6′-Me_2-2,2′-bpy ligand. The *ortho*-metalated carbide clusters react with terminal alkynes to give the alkenyl-substituted clusters $Ru_5(\mu_5\text{-}C)(CO)_{13}(\mu\text{-}RCHCHNNMe)$, establishing a viable cluster-based catalytic cycle for an alkyl-to-alkenyl functionalization of alkylated heterocyclic substrates.

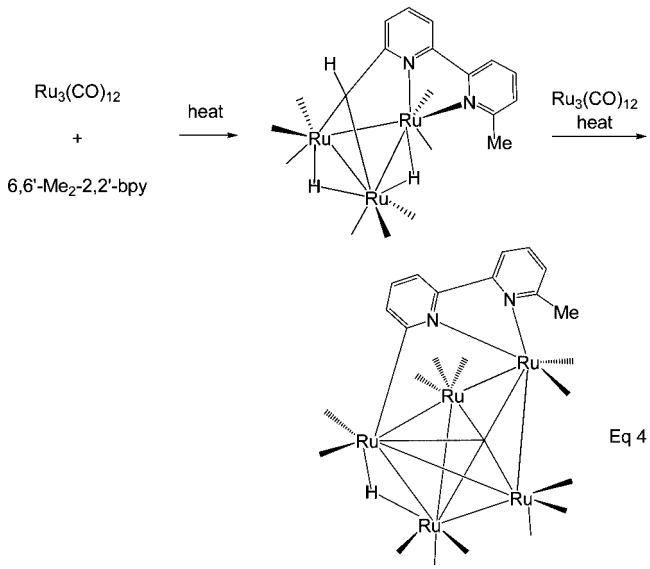

The coordination of the parent α-diimine ligands 2,2′-bpy and 1,10-phen at the trimetallic clusters $Ru_3(CO)_{12}$ and $Os_3(CO)_{12}$ gives the chelated clusters $Ru_3(CO)_{10}$(N-N) and $Os_3(CO)_{10}$(N-N),[4,5] whose ligand coordination sphere about the metallic polyhedron has been noted to be unduly crowded. This situation is further exacerbated by the presence of the two *ortho* methyl groups in the 6,6′-Me_2-2,2′-bipyridine and 2,9-Me_2-1,10-phenanthroline ligands and readily accounts for the absence of the putative cluster species $Ru_3(CO)_{10}$(6,6′-Me_2-2,2′-bpy) and $Ru_3(CO)_{10}$(2,9-Me_2-1,10-phen) in the Cabeza report. The extant steric crowding between the cluster-bound CO groups and the alkyl appendages of the heterocyclic auxiliary in these decacarbonyl clusters forms the basis for the chelate-directed C−H bond activation observed by Cabeza.

Given the steric-induced activation of the methyl groups in the *ortho*-disubstituted 2,2′-bpy ligand in the reactions depicted in eq 4, it seemed reasonable that reactions employing the slightly less encumbered heterocycle 6-Me-2,2′-bpy might facilitate the observation and isolation of the putative clusters $M_3(CO)_{10}$(6-Me-2,2′-bpy).[6] The conventional thermolysis conditions that are required to effect ligand substitution in the parent clusters $M_3(CO)_{12}$ (where M = Ru, Os) guarantee difficulty in the successful preparation of the target decacarbonyl clusters due to low-energy manifolds involving additional CO loss and metal skeletal reorganizations. The use of an activated cluster platform, one that would allow the substitution of the 6-Me-2,2′-bpy to occur at or near room temperature, could, in theory, allow the initial coordination chemistry to be established. Accordingly, we have selected $Os_3(CO)_{10}(MeCN)_2$ as our starting cluster to probe the early stages of the substitution reaction with the 6-Me-2,2′-bpy ligand. This particular cluster has a rich chemical history because the two MeCN ligands are lightly bound and readily replaced by donor ligands, making it an ideal precursor for studies dealing with the early stages of substrate binding and ligand activation at an intact polynuclear entity.[7,8]

Herein we report our data on the room-temperature reaction of 6-Me-2,2′-bpy with $Os_3(CO)_{10}(MeCN)_2$, which affords the isomeric hydride clusters $HOs_3(CO)_9(\mu_2\text{-}CH_2N_2C_{10}H_7)$ (**2**) and $HOs_3(CO)_9(\mu_2\text{-}N_2C_{11}H_9)$ (**3**). Thermolysis of cluster **2** leads to the formation of **3** (major) and the dihydride cluster $H_2Os_3(CO)_8(\mu_3\text{-}N_2C_{11}H_8)$ (**4**) (minor). The new clusters **2**−**4** have been isolated and fully characterized in solution and by X-ray crystallography. The dynamics associated with the reductive coupling of the cyclometalated methyl group and the bridging hydride in **2** have been kinetically probed in the presence of trapping ligands.

Experimental Section

General Methods. $Os_3(CO)_{12}$ was prepared by high-pressure carbonylation of OsO_4 using a 450 mL Parr Series 4560 benchtop-mini reactor,[9] with $Os_3(CO)_{10}(MeCN)_2$ synthesized from $Os_3(CO)_{12}$,

(3) (a) Cabeza, J. A.; da Silva, I.; del Río, I.; Martínez-Méndez, L.; Miguel, D.; Riera, V. I. *Angew. Chem., Int. Ed.* **2004**, *43*, 3464. (b) Cabeza, J. A.; del Río, I.; Martínez-Méndez, L.; Miguel, D. *Chem.−Eur. J.* **2006**, *12*, 1529.

(4) (a) Venalainen, T.; Pursiainen, J.; Pakkanen, T. A. *J. Chem. Soc., Chem. Commun.* **1985**, 1348. (b) Bruce, M. I.; Humphrey, M. G.; Snow, M. R.; Tiekink, E. R. T.; Wallis, R. C. *J. Organomet. Chem.* **1986**, *314*, 311. (c) Leadbeater, N. E.; Raithby, P. R.; Ward, G. N. *J. Chem. Soc., Dalton Trans.* **1997**, 2511. (d) Poola, B.; Wang, X.; Richmond, M. G. *J. Chem. Crystallogr.* **2007**, *37*, 641.

(5) For a report on the ligand-activated cluster $HOs_3(CO)_9(\mu\text{-}C_{10}H_7N_2)$, which has been isolated from the extended thermolysis of $Os_3(CO)_{10}$(2,2′-bpy), see:Deeming, A. J.; Peters, R.; Hursthouse, M. B.; Backer-Dirks, J. D. J. *J. Chem. Soc., Dalton Trans.* **1982**, 787.

(6) Whereas the reaction chemistry of mononuclear metal compounds with *ortho*-substituted 2,2′-bpy and 1,10-phen derivatives has been extensively investigated, the reactivity of metal clusters with the same ligands remains, to our knowledge, relatively unexplored. For some representative examples involving mononuclear systems, see:(a) Newkome, G. R.; Evans, D. W.; Kiefer, G. E.; Theriot, K. J. *Organometalllics* **1988**, *7*, 2537. (b) Constable, E. C.; Henney, R. P. G.; Leese, T. A.; Tocher, T. A. *J. Chem. Soc., Dalton Trans.* **1990**, 443. (c) Zucca, A.; Stoccoro, S.; Cinellu, M. A.; Minghetti, G.; Manassero, M. *J. Chem. Soc., Dalton Trans.* **1999**, 3431. (d) Romeo, R.; Plutino, M. R.; Scolaro, L. M.; Stoccoro, S.; Minghetti, G. *Inorg. Chem.* **2000**, *39*, 4749.

(7) (a) Burgess, K.; Johnson, B. F. G.; Lewis, J. *J. Organomet. Chem.* **1982**, *233*, C55. (b) Dahlinger, K.; Poë, A. J.; Sayal, P. K.; Sekhar, V. C. *J. Chem. Soc., Dalton Trans.* **1986**, 2145. (c) Zoet, R.; van Koten, G.; Vrieze, K.; Duisenberg, A. J. M.; Spek, A. L. *Inorg. Chim. Acta* **1988**, *148*, 71. (d) Akther, J.; Azam, K. A.; Das, A. R.; Hursthouse, M. B.; Kabir, S. E.; Abdul Malik, K. M.; Rosenberg, E.; Tesmer, M.; Vahrenkamp, H. *J. Organomet. Chem.* **1999**, *588*, 211. (e) Watson, W. H.; Poola, B.; Richmond, M. G. *J. Organomet. Chem.* **2006**, *691*, 4676.

(8) For a computational study dealing with the lability and isomerization of the MeCN ligands in $Os_3(CO)_{10}(MeCN)_2$, see:Musaev, D. G.; Nowroozi-Isfahani, T.; Morokuma, K.; Rosenberg, E. *Organometallics* **2005**, *24*, 5973.

(9) Drake, S. R.; Loveday, P. A. *Inorg. Synth.* **1990**, *28*, 230.

MeCN, and Me_3NO.[10] The heterocyclic ligand 6-Me-2,2′-bpy was prepared from 2,2′-bpy and MeLi,[11] while the 6-Me-d_3-2,2′-bpy ligand was prepared from 2,2′-bpy and Me-d_3-Li.[12] The deuterated ligand $P(OCD_3)_3$ was prepared according to the published procedure starting from CD_3OD (99.8 atom % D) and PCl_3.[13] The chemicals 2,2′-bpy, MeLi (1.6 M in Et_2O), Me-d_3-Li (99 atom % D; 0.5 M in Et_2O), and $Me_3NO\cdot 2H_2O$ were purchased from Aldrich Chemical Co. and used as received, except for the latter chemical, which was rendered anhydrous by azeotropic distillation from benzene. The alkyllithium reagents were titrated against diphenylacetic acid prior to use.[14] All reaction solvents were distilled from an appropriate drying agent under argon using Schlenk techniques and stored in Schlenk storage vessels equipped with high-vacuum Teflon stopcocks.[15] The solvents used in the collection of routine IR and NMR spectra were reagent grade and were typically degassed by three pump−thaw−degas cycles prior to their use. The solvents employed in all kinetic experiments were rigorously purified by bulb-to-bulb distillation from an appropriate drying agent prior to use. The photochemical studies were conducted with GE blacklight bulbs that had a maximum output at 366 ± 20 nm and a photon flux of ca. 1×10^{-6} einstein/min. The reported combustion analyses were performed by Atlantic Microlab, Norcross, GA.

The infrared spectra were recorded on a Nicolet 20 SXB FT-IR spectrometer in a 0.1 mm NaCl cell, using PC control and OMNIC software. The reported ^1H and ^{31}P NMR spectra were recorded at 200 MHz on a Varian Gemini-200 spectrometer and 121 MHz on a Varian 300-VXR spectrometer, respectively. The reported ^{31}P chemical shifts, which were recorded in the proton-decoupled mode, are referenced to external H_3PO_4 (85%), taken to have $\delta = 0$. The reported FAB and ESI mass spectral data were collected at the mass spectrometry facility at the University of California at San Diego. The ESI mass spectrum was recorded in the positive ion mode using MeOH and a trace amount of AcOH as the sample matrix, while the FAB mass spectra were recorded using 3-nitrobenzyl alcohol as the sample matrix. The GC-MS data on the ligands 6-Me-2,2′-bpy and 6-Me-d_3-2,2′-bpy were recorded on a Finnigan/Thermo-Electron GC-MS system at UNT.

Preparation of the Hydride-Bridged Clusters $HOs_3(CO)_9(\mu_2\text{-}CH_2N_2C_{10}H_7)$ (2) and $HOs_3(CO)_9(\mu_2\text{-}N_2C_{11}H_9)$ (3) from $Os_3(CO)_{10}(MeCN)_2$ (1) and 6-Me-2,2′-bpy. To an argon-filled Schlenk flask containing 0.30 g (0.32 mmol) of cluster **1** was added 100 mL of CH_2Cl_2 via cannula, followed by 54 mg (0.32 mmol) of 6-Me-2,2′-bpy. The reaction was stirred for 2 h at room temperature and then examined by TLC analysis, which confirmed the consumption of the starting cluster and the presence of clusters **2** and **3** as two close running spots [$R_f = 0.50$ for **3** and $R_f = 0.45$ for **2** in CH_2Cl_2/hexane (1:1)]. A considerable amount of decomposed material also accompanied the reaction based on the dark brown spot that remained at the origin of the TLC plate. The solvent was next evaporated, and the desired clusters **2** and **3** were isolated by column chromatography over silica gel. Cluster **3** was obtained by using CH_2Cl_2/hexane (1:3) as the eluent, with cluster **2** eluting when the mobile phase was changed to a 3:7 mixture of CH_2Cl_2/hexane. Crude yield of cluster **3**: 9.4% (30 mg). Cluster **2** was recrystallized from benzene/CH_2Cl_2 to furnish **2** as a red-orange solid in 38% yield (0.12 g). Data for **2**: IR (CH_2Cl_2): ν(CO) 2075 (s), 2030 (vs), 2008 (vs), 1987 (s), 1967 (s), 1946 (s) cm^{-1}. ^1H NMR (CD_2Cl_2): δ 9.27 (d, 1H, $J = 5$ Hz), 8.08 (d, 1H, $J = 8$ Hz), 7.95−7.80 (m, 2H), 7.53−7.24 (m, 3H), 2.87 (multiplet, CH_2 group, $^1J = 16$ Hz, $^3J = 3$ Hz, $^3J = 1$ Hz), −20.25 (s, hydride). Anal. Calc (Found) for $C_{20}H_{10}N_2O_9Os_3\cdot 1/4C_6H_6$: C, 25.48 (25.06); H, 1.14 (1.22).

Preparation of $HOs_3(CO)_9(\mu_2\text{-}N_2C_{11}H_9)$ (3) and $H_2Os_3(CO)_8(\mu_3\text{-}N_2C_{11}H_8)$ (4) from the Thermolysis of $HOs_3(CO)_9(\mu_2\text{-}CH_2N_2C_{10}H_7)$ (2). To 0.10 g (0.10 mmol) of cluster **2** in a Schlenk tube under argon flush was added 40 mL of toluene via syringe, after which the vessel was capped and placed in a thermostated bath at 75 °C. The solution was heated for 24 h, with periodic monitoring by TLC analysis. The cooled solution revealed the presence of two closely moving spots by TLC corresponding to cluster **3** ($R_f = 0.50$) and the dihydride cluster **4** ($R_f = 0.47$) using a 1:1 mixture of CH_2Cl_2/hexane as the eluent. The toluene was removed under vacuum and the residue subjected to column chromatography using the aforementioned mobile phase. Both product clusters **3** and **4** were subsequently recrystallized from benzene/hexane to furnish **3** as a red-orange solid (70 mg; 70% yield) and **4** as a yellow-orange solid (21 mg; 22% yield). Cluster **3**: IR (CH_2Cl_2): ν(CO) 2083 (s), 2041 (vs), 2003 (vs), 1987 (s), 1955 (s), 1933 (m) cm^{-1}. ^1H NMR (CD_2Cl_2): δ 8.10 (d, 1H, $J = 8$ Hz), 7.71 (t, 1H, $J = 8$ Hz), 7.45−7.10 (m, 4H), 2.80 (s, 3H, Me), −21.48 (s, hydride). Anal. Calc (Found) for $C_{20}H_{10}N_2O_9Os_3$: C, 24.19 (24.38); H, 1.02 (1.49). Cluster **4**: IR (CH_2Cl_2): ν(CO) 2089 (s), 2049 (vs), 2004 (vs), 1985 (s), 1970 (s), 1950 (m), 1923 (m) cm^{-1}. ^1H NMR (CD_2Cl_2): δ 9.09 (d, 1H, $J = 5$ Hz), 7.90 (m, 1H), 7.50 (t, 1H, $J = 8$ Hz), 7.38−7.28 (m, 2H), 7.18 (d, 1H, $J = 8$ Hz), 6.97 (d, 1H, $J = 8$ Hz), 5.38 (s, 1H, carbyne CH), −10.81 (d, 1H, $J = 2$ Hz), −14.82 (d, 1H, $J = 2$ Hz). Anal. Calc (Found) for $C_{19}H_{10}N_2O_8Os_3$: C, 23.63 (23.91); H, 1.04 (1.45).

Photochemical Preparation of Cluster 4 from Cluster 2. Here the reaction was conducted in a NMR tube that was equipped with a J-Young valve in order to release the liberated CO that accompanies the formation of cluster **4**. The NMR tube was charged with 50 mg (0.050 mmol) of cluster **2** and 0.7 mL of benzene-d_6, after which the tube was subjected to three freeze−pump−thaw degas cycles. The photolysis was carried out using two GE blacklights, and the progress of the reaction was assessed by ^1H NMR spectroscopy. Quantitative conversion of **2** to **4** was realized after several days of continuous photolysis. The time for the reaction was not optimized, as it is dependent on the removal of the liberated CO, which in turn depends on the number of additional freeze−pump−thaw degas cycles. Typically, the NMR tube was subjected to one freeze−pump−thaw degas cycle per day.

Preparation of 6-Me-d_3-2,2′-bpy from 2,2′-bpy and Me-d_3-Li. To 5.0 g (0.032 mol) of 2,2′-bpy in 250 mL of Et_2O at 0 °C was added 64 mL of a 0.5 M ether solution (0.032 mol) of Me-d_3-Li dropwise via a pressure-equalizing addition funnel. The temperature was maintained at 0 °C during the addition phase of Me-d_3-Li to the reaction, after which the reaction solution was allowed to warm to room temperature with continuous stirring. At this point the resulting maroon solution was refluxed for ca. 3 h, followed by cooling and quenching with 30 mL of water. The organic layer was separated via cannula and the aqueous layer extracted with 3 × 20 mL portions of Et_2O. The combined organic layers were dried over sodium sulfate and filtered, and the solvent was removed under vacuum to afford the corresponding dihydro adduct 6-methyl-d_3-1,6-dihydro-2,2′-bipyridine, which was then oxidized by using 300 mL of a saturated $KMnO_4$ solution in acetone. The accompanying MnO_2 was filtered away and the acetone removed under vacuum to furnish a dark red liquid, which was passed across a column of neutral alumina using Et_2O/hexane (1:4) as the eluent. The desired ligand 6-Me-d_3-2,2′-bpy was obtained as a colorless oily liquid in 70% yield (3.9 g). ^1H NMR (CD_2Cl_2): δ 8.67 (d, 1H, $J = 5$ Hz), 8.42 (dt, 1H, $J = 8$ Hz, $J = 2$ Hz), 8.18 (d, 1H, $J = 8$ Hz), 7.81 (dt, 1H, $J = 8$ Hz, $J = 2$ Hz),

(10) Nicholls, J. N.; Vargas, M. D. *Inorg. Synth.* **1989**, *26*, 289.
(11) Schmalzl, K. J.; Summers, L. A. *Aust. J. Chem.* **1977**, *30*, 657.
(12) Garber, T.; Van Wallendael, S.; Rillema, D. P.; Kirk, M.; Hatfield, W. E.; Welch, J. H.; Singh, P. *Inorg. Chem.* **1990**, *29*, 2863.
(13) Ferrari, A.; Polo, E.; Rüegger, H.; Sostero, S.; Venanzi, L. M. *Inorg. Chem.* **1996**, *35*, 1602.
(14) Kofron, W. G.; Baclawski, L. M. *J. Org. Chem.* **1976**, *41*, 1879.
(15) Shriver, D. F. *The Manipulation of Air-Sensitive Compounds*; McGraw-Hill: New York, 1969.

7.71 (t, 1H, $J = 8$ Hz), 7.30 (ddd, 1H, $J = 8$ Hz, $J = 5$ Hz, $J = 1$ Hz), 7.18 (dd, 1H, $J = 8$ Hz, $J = 1$ Hz). GC-MS: *m/z* 173.0 $[M]^+$.

Preparation of the Deuteride-Bridged Cluster $DOs_3(CO)_9(\mu_2\text{-}CD_2N_2C_{10}H_7)$ (2-d_3) and the Hydride-Bridged Cluster $HOs_3(CO)_9(\mu_2\text{-}N_2C_{11}H_6D_3)$ (3-d_3) from $Os_3(CO)_{10}(MeCN)_2$ (1) and 6-Me-d_3-2,2′-bpy. The procedure employed for the preparation of the d_3-isotopomers parallels that reported above for clusters **2** and **3** using 6-Me-2,2′-bpy. Here an argon-filled Schlenk flask containing 0.30 g (0.32 mmol) of cluster **1** dissolved in 100 mL of CH_2Cl_2 was treated with 55 mg (0.32 mmol) of 6-Me-d_3-2,2′-bpy. The reaction was stirred for ca. 2 h at room temperature, after which time TLC analysis confirmed the presence of the desired clusters **2**-d_3 and **3**-d_3. The solvent was evaporated, and both product clusters were isolated by column chromatography over silica gel. Cluster **3**-d_3 was obtained by using CH_2Cl_2/hexane (1:3) as the eluent, followed by cluster **2**-d_3 when the mobile phase was changed to a 3:7 mixture of CH_2Cl_2/hexane. Both products were recrystallized from benzene/CH_2Cl_2 to furnish cluster **3**-d_3 in 18% yield (58 mg) and cluster **2**-d_3 in 29% yield (93 mg). Data for **2**-d_3: IR (CH_2Cl_2): ν(CO) 2075 (s), 2028 (vs), 2004 (vs), 1986 (s), 1970 (s), 1947 (s) cm^{-1}. ^1H NMR (CD_2Cl_2): δ 9.27 (d, 1H, $J = 5$ Hz), 8.08 (d, 1H, $J = 8$ Hz), 7.92 (d, 1H, $J = 8$ Hz), 7.80 (d, 1H, $J = 6$ Hz), 7.53−7.24 (m, 3H). FAB-MS: *m/z* 997.2 (calcd for $[M + H]^+$: $C_{20}H_8D_3N_2O_9Os_3$ 997.0), along with ions for the sequential loss of seven CO groups. Data for Cluster **3**-d_3: IR (CH_2Cl_2): ν(CO) 2084 (s), 2040 (vs), 2005 (vs), 1985 (s), 1955 (s), 1932 (m) cm^{-1}. ^1H NMR (CD_2Cl_2): δ 8.10 (d, 1H, $J = 8$ Hz), 7.71 (t, 1H, $J = 8$ Hz), 7.45−7.10 (m, 4H), −21.48 (s, hydride). FAB-MS: *m/z* 997.2 (calcd for $[M + H]^+$: $C_{20}H_8D_3N_2O_9Os_3$ 997.0), along with ions for the sequential loss of five CO groups.

Synthesis of $HOs_3(CO)_9[P(OMe)_3](\mu_2\text{-}N_2C_{11}H_9)$ (5) from Cluster 3 and $P(OMe)_3$. To a large Schlenk tube containing 0.10 g of **3** (0.10 mmol) and 50 mL of toluene was added 0.12 mL (1.0 mmol) of $P(OMe)_3$ via syringe. The vessel was then heated at ca. 60 °C and monitored by TLC analysis until the starting cluster was consumed, after which time the solvent and the excess $P(OMe)_3$ were removed under vacuum. The yellow residue was then passed across a short column of silica gel using CH_2Cl_2 as the eluent and then recrystallized from benzene/CH_2Cl_2 to afford 84 mg (75% yield) of yellow **5**. IR (CH_2Cl_2): ν(CO) 2086 (s), 2043 (vs), 2019 (vs), 1997 (vs), 1979 (sh), 1963 (s), 1920 (w) cm^{-1}. ^1H NMR (CD_2Cl_2): δ 7.55 (t, 1H, $J = 7$ Hz), 7.18−6.90 (m, 4H), 6.50 (d, 1H, J 7 Hz), 3.59 and 3.39 (d, methoxy groups, $J = 12$ Hz, 30% and 70%, respectively), 2.54 and 2.43 (s, 6-Me groups, 30% and 70%, respectively), −14.62 and −14.80 (d, hydrides, $J_{P-H} = 11$ Hz for both, 30% and 70%, respectively). ^{31}P NMR (CD_2Cl_2): δ 114.08 and 116.25 (s, 30% and 70%, respectively). ESI-MS: *m/z* 1118.57 (calcd for $[M + H]^+$: $C_{23}H_{20}N_2O_{12}Os_3P$ 1118.07), along with ions for the loss of one and three CO groups.

Kinetics Studies. The UV−vis studies employed a cluster concentration of ca. 10^{-4} M using 1.0 cm quartz UV−visible cells that were equipped with a high-vacuum Teflon stopcock to facilitate handling on the vacuum line. Solutions of cluster **2** were prepared under either argon or CO (1 atm) and used immediately before each kinetic measurement. The experiments conducted with cluster **2** at high CO pressure were carried out in a carbon-steel 300 mL autoclave, whose internal CO pressure was kept constant with a Tescom pressure regulator. The autoclave was equipped with a tip tube that enabled sample removal for UV−vis analysis while maintaining constant CO pressure. The Hewlett-Packard 8452A diode array spectrometer employed in our studies was configured with a variable-temperature cell holder and was connected to a VWR constant-temperature circulator, allowing for the quoted temperatures to be maintained within ±0.5 K. The UV−vis kinetics for the reaction of cluster **2** in the presence of ligand-trapping agents were monitored by following the decrease of the 540 nm absorbance band as a function of time for at least 4−6 half-lives. The kinetics for the reaction between cluster **3** with added ligand were followed similarly, using the 540 nm absorbance band of **3** to monitor the progress of the reaction. The UV−vis-derived rate constants quoted in Tables 3–5 were determined by nonlinear regression analysis using the single-exponential function[16] $A(t) = A_\infty + \Delta A e^{(-kt)}$.

The ^1H NMR kinetic experiments were conducted in 5 mm NMR tubes that possessed a J. Young value in CD_2Cl_2 solvent or in NMR tubes equipped with a right-angle high-vacuum Teflon stopcock. These latter NMR tubes were manipulated on the vacuum line and then flamed sealed after multiple freeze−pump−thaw degassing cycles. The NMR reactions were followed for a period of 2−3 half-lives, and the extent of these reactions was determined by calibration against a measured amount of the internal standard ferrocene. The rate constants quoted from the NMR experiments were determined by traditional graphical analysis of ln[cluster] versus time plots.

The activation parameters for the consumption of clusters **2** and **3** in the ligand reactivity studies were calculated from a plot of $\ln(k/T)$ versus T^{-1},[17] with the error limits representing the deviation of the data points about the least-squares line of the Eyring plot.

X-ray Structural Analyses. Single crystals of clusters **2**−**4** suitable for X-ray crystallography were grown from CH_2Cl_2 and hexane. The X-ray data were collected on a Bruker X8 APEX CCD diffractometer using Mo radiation and a graphite monochromator. The frames were integrated with the available SAINT software package using a narrow-frame algorithm,[18] with each structure solved and refined using the SHELXTL program package.[19] The molecular structures were checked by using PLATON,[20] and all non-hydrogen atoms were refined anisotropically, with the carbon-bound hydrogens assigned to calculated positions and allowed to ride on the attached carbon atom. The bridging hydrides in the three structures were not located during refinement. Tables 1 and 2 summarize the pertinent X-ray data for these clusters.

Results and Discussion

I. Reaction of 1,2-$Os_3(CO)_{10}(MeCN)_2$ with 6-Me-2,2′-bpy. Treatment of 1,2-$Os_3(CO)_{10}(MeCN)_2$ with an equimolar amount of 6-Me-2,2′-bpy in CH_2Cl_2 at room temperature furnishes the isomeric hydride-bridged clusters $HOs_3(CO)_9(\mu_2\text{-}CH_2N_2C_{10}H_7)$ (**2**) and $HOs_3(CO)_9(\mu_2\text{-}N_2C_{11}H_9)$ (**3**). The expected precursor to **2** and **3**, namely, the ligand-chelated cluster $Os_3(CO)_{10}(\mu$-6-Me-2,2′-bpy), was not observed at any time when our reactions were monitored by TLC and IR and ^1H NMR spectroscopies (*vide infra*) at room temperature. This indicates that once formed, the logical intermediate must undergo rapid cyclometalation and *ortho* metalation to afford clusters **2** and **3**, respectively. A control experiment involving the reaction of 1,2-$Os_3(CO)_{10}(MeCN)_2$ with 6-Me-2,2′-bpy in $CDCl_3$ was performed at −20 °C, in an effort to trap the putative cluster $Os_3(CO)_{10}(\mu$-6-Me-2,2′-bpy). No reaction was observed over the course of 2 days at this temperature when monitored by ^1H NMR spectroscopy. Raising the temperature to 0 °C led to the release of MeCN (δ 2.08) and formation of a new species exhibiting ^1H resonances at δ 9.48 (1H, d, $J = 6$ Hz), 8.20−7.40 (6H, overlapping bpy hydrogens), and 2.90 (3H, s, Me), whose

(16) The rate calculations were performed by using the commercially available program Origin6.0. Here the initial (A_o) and final (A_∞) absorbances and the rate constant were floated to give the quoted least-squares value for the first-order rate constant *k*.

(17) Carpenter, B. K. *Determination of Organic Reaction Mechanisms*; Wiley-Interscience: New York, 1984.

(18) *SAINT*, Version 6.02; Bruker Analytical X-ray Systems, Inc.: Madison, WI, 1997−1999.

(19) *SHELXTL*, Version 5.1; Bruker Analytical X-ray Systems, Inc.: Madison, WI, 1998.

(20) Spek, A. L. *PLATON-A Multipurpose Crystallographic Tool*; Utrecht University: Utrecht, The Netherlands, 2001.

Table 1. X-ray Crystallographic Data and Processing Parameters for the Triosmium Clusters 2−4

	2	3	4
CCDC entry no.	626670	626671	626669
T, K	240 (2)	298 (2)	220 (2)
cryst syst	triclinic	triclinic	triclinic
space group	$P\bar{1}$	$P\bar{1}$	$P\bar{1}$
a, Å	9.840(1)	8.5944(4)	8.4706(7)
b, Å	9.957(1)	8.8308(4)	10.3476(8)
c, Å	12.684(2)	15.3940(7)	12.451(1)
α, deg	82.793(6)	82.301(2)	89.440(4)
β, deg	82.191(6)	86.900(2)	80.517(4)
γ, deg	67.556(6)	79.624(2)	89.108(4)
V, Å^3	1134.3(2)	1138.33(9)	1076.2(2)
mol formula	$C_{20}H_{10}N_2Os_3O_9$	$C_{20}H_{10}N_2Os_3O_9$	$C_{19}H_{10}N_2Os_3O_8$
fw	992.89	992.89	964.87
formula units per cell (Z)	2	2	2
D_{calcd} (Mg/m^3)	2.904	2.894	2.968
λ(Mo Kα), Å	0.71073	0.71073	0.71073
absorp coeff (mm^{-1})	16.816	16.756	17.714
R_{merge}	0.0573	0.0504	0.0361
abs corr, max./min.	SADABS, 0.2841/0.0812	SADABS, 0.0815/0.0355	SADABS, 0.4712/0.0761
total no. of reflns	33 023	26 223	35 753
no. of indep reflns	11 343	10 435	11 183
no. of data/restr/params	11 343/0/307	10 35/0/307	11 183/0/284
R	0.0441	0.0583	0.0240
R_w	0.1099	0.1363	0.0516
GOF on F^2	0.976	1.003	1.008
Δρ(max.), Δρ(min.) (e^3)	3.237, −2.815	5.150, −5.446	1.479, −1.832

integral ratios are consistent with the proposed Os_3 cluster containing an ancillary 6-Me-2,2′-bpy ligand. $Os_3(CO)_{10}(\mu$-6-Me-2,2′-bpy) is not stable at this temperature and undergoes competitive conversion to the hydride clusters **2** and **3**. The latter products, whose structures are shown below, were subsequently isolated by careful column chromatography as red-orange, relatively air-stable solids.

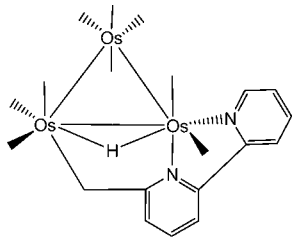

cluster **2**

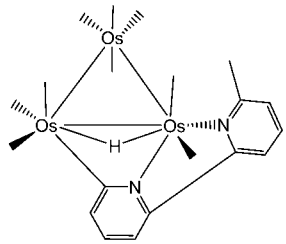

cluster **3**

The ^{1}H NMR spectrum for **2** exhibits its seven aromatic hydrogens as multiple resonances over the region δ 9.27−7.24, of which the downfield doublet at δ 9.27 is readily assigned to the *ortho* hydrogen or 6′ hydrogen on the unsubstituted bipyridyl ring.[21] Cyclometalation of the original 6-Me group affords a methylene moiety centered at δ 2.87 and a slightly broadened high-field hydride resonance at δ −20.25. The observed broadening in the high-field hydride is ascribed to small but finite couplings with the diastereotopic methylene hydrogens, as verified by spectral simulation of these three hydrogens within an ABX spin system. The thermal ellipsoid plot of **2** shown in Figure 1 confirms the chelation of the bpy moiety and the cyclometalation of the methyl carbon C(30) to the Os(2) and Os(1) centers, respectively. The Os−Os bond distances range from 2.9100(4) Å [Os(1)−Os(2)] to 2.9033(4) Å [Os(2)−Os(3)], with an average distance of 2.9065 Å. While the hydride ligand was not located during refinement, it is confidently assigned to the Os(1)−Os(2) vector on the basis of structural trends found in related osmium clusters.[22] The Os(1)−C(30) bond length of 2.245(6) Å is in good agreement with those distances reported in analogous cyclometalated Os_3 derivatives.[23]

Cluster **3** was fully characterized in solution by IR and ^{1}H NMR spectroscopies, and the molecular structure determined by X-ray

Table 2. Selected Bond Distances (Å) and Angles (deg) for the Triosmium Clusters 2−4

Cluster 2			
Bond Distances			
Os(1)−Os(2)	2.9100(5)	Os(1)−Os(3)	2.9063(4)
Os(2)−Os(3)	2.9033(4)	Os(1)−C(7)	1.889(6)
Os(1)−C(8)	1.943(7)	Os(1)−C(9)	1.904(6)
Os(1)−C(30)	2.245(6)	Os(2)−N(1)	2.138(5)
Os(2)−N(2)	2.092(5)	Os(2)−C(1)	1.866(7)
Os(2)−C(2)	1.898(6)	Os(3)−C(3)	1.892(7)
Os(3)−C(4)	1.962(7)	Os(3)−C(5)	1.907(6)
Os(3)−C(6)	1.928(6)	C(11)−C(30)	1.466(9)
Bond Angles			
Os(2)−Os(1)−C(8)	101.43(2)	Os(3)−Os(1)−C(8)	83.4(2)
Os(2)−Os(1)−C(30)	77.6(2)	Os(2)−Os(1)−C(7)	117.6(2)
Os(1)−Os(2)−C(2)	113.3(2)	Os(1)−Os(2)−N(1)	84.9(1)
Os(1)−Os(2)−N(2)	148.2(2)	N(1)−Os(2)−N(2)	77.1(2)
Os(2)−N(1)−C(11)	123.8(4)	Os(2)−N(1)−C(15)	115.5(4)
Os(2)−N(2)−C(16)	117.2(4)	Os(2)−N(2)−C(20)	124.9(4)
Os(3)−Os(1)−C(30)	102.3(2)	Os(3)−Os(2)−N(1)	85.6(1)
Cluster 3			
Bond Distances			
Os(1)−Os(2)	2.8910(5)	Os(1)−Os(3)	2.8915(5)
Os(2)−Os(3)	2.8933(5)	Os(1)−C(7)	1.89(1)
Os(1)−C(8)	1.94(1)	Os(1)−C(9)	1.90(1)
Os(1)−C(20)	2.13(1)	Os(2)−N(1)	2.179(9)
Os(2)−N(2)	2.057(9)	Os(1)−C(1)	1.89(1)
Os(2)−C(2)	1.86(1)	Os(3)−C(3)	1.90(1)
Os(3)−C(4)	1.94(1)	Os(3)−C(5)	1.92(1)
Os(3)−C(6)	1.94(1)		
Bond Angles			
Os(2)−Os(1)−C(8)	104.8(4)	Os(3)−Os(1)−C(8)	89.5(4)
Os(2)−Os(1)−C(20)	68.8(3)	Os(2)−Os(1)−C(7)	116.0(4)
Os(1)−Os(2)−C(2)	109.0(3)	Os(1)−Os(2)−N(1)	137.3(2)
Os(1)−Os(2)−N(2)	68.4(2)	N(1)−Os(2)−N(2)	75.1(3)
Os(2)−N(2)−C(20)	114.2(7)	Os(2)−N(2)−C(16)	121.4(7)
Os(2)−N(1)−C(15)	111.1(6)	Os(2)−N(1)−C(11)	128.1(8)
Os(3)−Os(1)−C(20)	89.2(3)	Os(3)−Os(2)−N(2)	84.9(2)
Cluster 5			
Bond Distances			
Os(1)−Os(2)	2.9556(3)	Os(1)−Os(3)	2.7984(3)
Os(2)−Os(3)	2.7745(3)	Os(1)−C(7)	1.892(4)
Os(1)−C(8)	1.940(4)	Os(1)−C(9)	1.904(3)
Os(1)−C(10)	2.185(3)	Os(2)−N(1)	2.102(2)
Os(2)−N(2)	2.160(2)	Os(2)−C(1)	1.861(3)
Os(2)−C(2)	1.888(3)	Os(3)−C(3)	1.893(3)
Os(3)−C(4)	1.926(3)	Os(3)−C(5)	1.914(4)
Os(3)−C(10)	2.165(3)		
Bond Angles			
Os(2)−Os(1)−C(8)	97.8(1)	Os(2)−Os(1)−C(10)	72.75(8)
Os(3)−Os(1)−C(8)	117.5(1)	Os(3)−Os(1)−C(9)	97.5(1)
C(7)−Os(1)−C(10)	93.5(1)	C(8)−Os(1)−C(9)	94.2(2)
C(8)−Os(1)−C(10)	166.7(1)	C(9)−Os(1)−C(10)	91.4(2)
Os(2)−Os(1)−C(7)	109.1(1)	Os(1)−Os(3)−C(4)	118.81(8)
Os(1)−Os(3)−C(3)	94.0(1)	Os(2)−Os(3)−C(4)	91.05(9)
Os(2)−Os(3)−C(10)	76.98(8)	C(3)−Os(3)−C(10)	90.4(1)
Os(1)−Os(2)−N(1)	80.89(6)	Os(1)−Os(2)−N(2)	122.57(6)
Os(3)−Os(2)−N(1)	86.46(6)	Os(3)−Os(2)−N(2)	160.59(6)
N(1)−Os(2)−N(2)	75.04(9)	N(1)−Os(2)−C(1)	169.4(1)
N(1)−Os(2)−C(2)	100.0(1)	N(2)−Os(2)−C(1)	104.9(1)
Os(1)−C(10)−Os(3)	80.07(8)	N(1)−C(11)−C(10)	117.8(2)

(21) (a) Anderson, S.; Constable, E. C.; Seddon, K. R.; Turp, J. E.; Baggott, J. E.; Pilling, M. J. *J. Chem. Soc., Dalton Trans.* **1985**, 2247. (b) Prasad, R.; Kumar, A.; Kumar, R. *J. Mol. Struct.* **2006**, *786*, 68.

(22) (a) Watson, W. H.; Poola, B.; Richmond, M. G. *Polyhedron* **2007**, *26*, 3585. (b) Liu, Y.-C.; Yeh, W.-Y.; Lee, G.-H.; Peng, S.-M. *J. Organomet. Chem.* **2005**, *690*, 163.

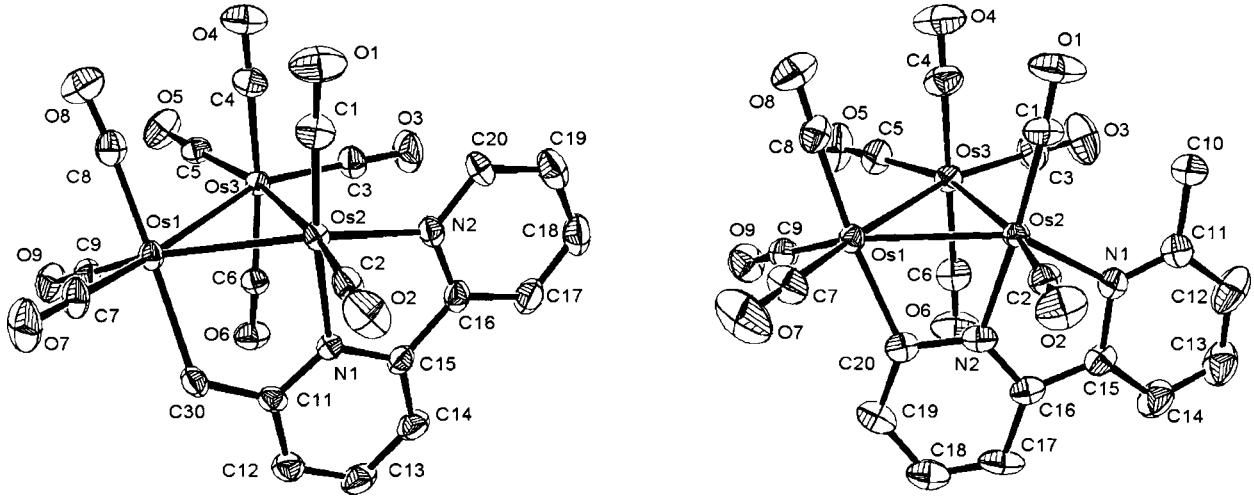

Figure 1. Thermal ellipsoid plots of the triosmium clusters **2** (left) and **3** (right) showing the thermal ellipsoids at the 40% probability level.

crystallography. The *ortho* metalation attendant in **3** was initially confirmed by ^{1}H NMR spectroscopy, where three sets of aromatic hydrogens that integrated for a total of six hydrogens were observed from δ 8.10 to 7.10, along with methyl and hydride singlets recorded at δ 2.80 and −21.48, respectively. The thermal ellipsoid plot of **3** shown in Figure 1 establishes the oxidative coupling of the 6′ hydrogen on the unsubstituted bipyridyl ring, and with it the formation of the four-membered metallocyclic ring composed by the atoms Os(1)−Os(2)−N(2)−C(20). The Os−Os bond distances in **3** range from 2.8909(5) Å [Os(1)−Os(2)] to 2.8933(5) Å [Os(2)−Os(3)], exhibiting a mean length of 2.8919 Å. The bridging hydride ligand was not located but is assumed to bridge the Os(1)−Os(2) vector as the hydride ligand in those triosmium clusters possessing related $\mu_{2,3}$-bridging nitrogen ligands.[5,24] The N(1) and N(2) atoms are chelated to the Os(2) atom in what may be formally viewed as equatorial and axial sites, respectively. The Os(1)−C(20) bond distance of 2.13(1) Å is in concert with those distances found in the *ortho*-metalated bpy ligand in $HOs_3(CO)_9(\mu$-$C_{10}H_7N_2)$ and other Os_3 clusters with metalated nitrogenous ligands.[5,25]

II. Thermolysis and Photochemical Reactivity of Clusters 2 and 3. The possible interconversion between the isomeric clusters **2** and **3** was next examined by independent thermolysis and photolysis experiments. Here reductive coupling of the hydride ligand with the methylene moiety (in **2**) or the pyridyl ring (in **3**) could, in theory, furnish the common intermediate, namely, the unsaturated 46e$^-$ cluster $Os_3(CO)_9$(6-Me-2,2′-bpy), and allow us to probe the kinetic and thermodynamic relationship between the two isomeric clusters. Thermolysis of **2** in toluene at 75 °C led to the complete consumption of **2** and the formation of two products, with TLC analysis confirming the presence of cluster **3** as the major product of the mixture. Both products were subsequently isolated, and the minor product (cluster **4**) was characterized by spectroscopic methods and X-ray crystallography. The two doublets found at δ −10.81 and −14.82 in the ^{1}H NMR spectrum of **4** suggested the formation of dihydride species through an additional C−H bond activation process. That these hydrogens originated from the initial 6-Me group was corroborated by the observation of seven bipyridyl hydrogens over the region δ 9.09−6.97 in the ^{1}H NMR spectrum, of which the downfield doublet centered at δ 9.09 may be confidently ascribed to the 6′ hydrogen of the unsubstituted bipyridyl ring. The assignment of the remaining methine resonance at δ 5.38 is straightforward and matches those NMR data reported for the methine moieties in the structurally related dihydrides $H_2Ru_3(CO)_8(\mu_3$-HCN-NMe) (where N-N = 2,2′-bpy, 1,10-phen).[3] Photolysis of **2** at room temperature using near-UV light also gives cluster **4** slowly as the sole observable product, as shown in eq 5. Optical excitation in **2** promotes CO loss, followed by activation of the methylene group of the cyclometalated ring. Figure 2 shows the thermal ellipsoid plot of cluster **4** and confirms the formal loss of CO and the C−H

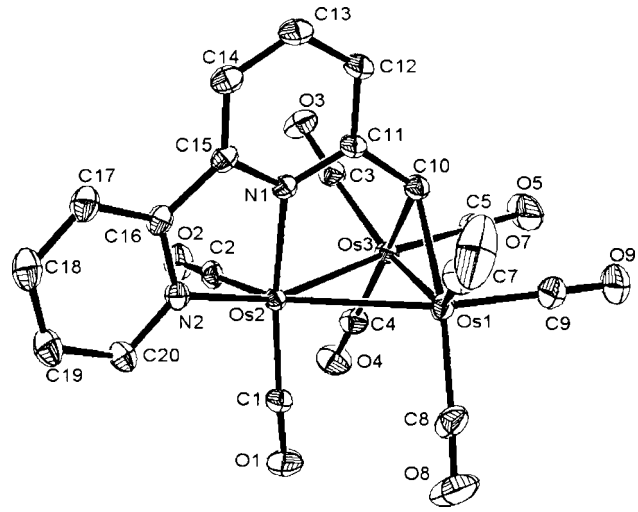

Figure 2. Thermal ellipsoid plot of the triosmium cluster **4** showing the thermal ellipsoids at the 40% probability level.

(23) (a) Zoet, R.; van Koten, G.; Vrieze, K.; Jansen, J.; Goubitz, K.; Stam, C. H. *Organometallics* **1988**, *7*, 1565. (b) Yeh, W.-Y.; Yang, C.-C.; Peng, S.-M.; Lee, G.-H. *J. Chem. Soc., Dalton Trans.* **2000**, 1649.

(24) (a) Day, M.; Espitia, D.; Hardcastle, K. I.; Kabir, S. E.; Rosenberg, E.; Gobetto, R.; Milone, L.; Osella, D. *Organometallics* **1991**, *10*, 3550. (b) Kabir, S. E.; Rosenberg, E.; Day, M.; Hardcastle, K.; Wolf, E.; McPhillips, T. *Organometallics* **1995**, *14*, 721. (c) Azam, K. A.; Das, A. R.; Hursthouse, M. B.; Kabir, S. E.; Malik, K. M. A. *J. Chem. Crystallogr.* **1998**, *28*, 283. (d) Wong, W.-Y.; Cheung, S.-H.; Huang, X.; Lin, Z. *J. Organomet. Chem.* **2002**, *655*, 39.

(25) (a) Au, Y.-K.; Cheung, K.-K.; Wong, W. T. *Inorg. Chim. Acta* **1995**, *238*, 193. (b) Deeming, A. J.; Stchedroff, M. J.; Whittaker, C.; Arce, A. J.; De Sanctis, Y.; Steed, J. W. *J. Chem. Soc., Dalton Trans.* **1999**, 3289. (c) Wong, W.-Y.; Cheung, S.-H.; Lee, S.-M.; Leung, S.-Y. *J. Organomet. Chem.* **2000**, *596*, 36. (d) Clarke, L. P.; Cole, J. M.; Davies, J. E.; French, A.; Koentjoro, O. F.; Raithby, P. R.; Shields, G. P. *New J. Chem.* **2005**, *29*, 145. (e) Machado, R. A.; Goite, M. C.; Arce, A. J.; De Sanctis, Y.; Deeming, A. J.; D'Ornelas, L.; Oliveros, D. A. *J. Organomet. Chem.* **2005**, *690*, 622.

bond activation in cluster **2**. Cluster **4** contains 48-valence electrons and is electron precise. The capping of one of the cluster faces by the six-electron 6-CH-2,2′-bpy ligand via both nitrogen atoms and a μ_2-carbene moiety and the presence of eight terminal CO groups are confirmed. The three Os−Os bond distances range from 2.7745(2) Å [Os(2)−Os(3)] to 2.9556(3) Å [Os(1)−Os(2)], with the hydrides presumed to bridge the Os(1)−Os(2) and Os(1)−Os(3) vectors in keeping with related Os_3 cluster analogues.[2a,3,23a,25d]

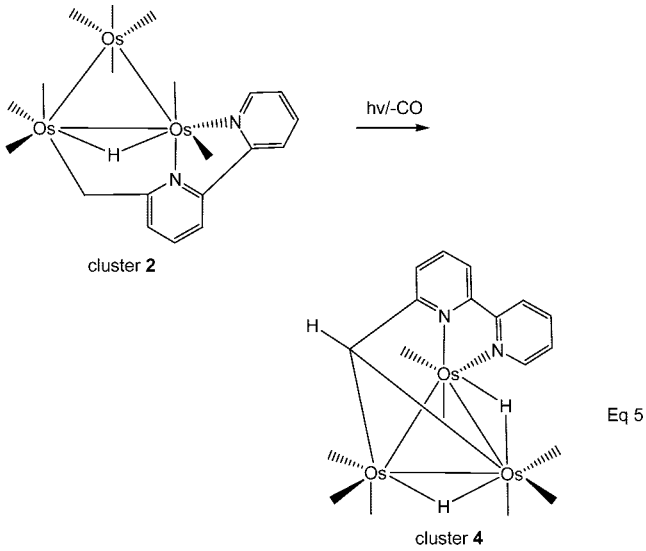

The thermal and photochemical reactivity of cluster **3** exhibits very different behavior in comparison to cluster **2**. Thermolysis of **3** in toluene at 75 °C revealed no perceptible changes when monitored by IR and TLC analyses over the course of 24 h, establishing cluster **3** as the thermodynamically more stable cluster in the isomeric pair of monohydrides. The photochemical sensitivity of **3** was also probed, and only a slow bleaching of the cluster was observed by UV−vis spectroscopy over the course of several days.

III. Kinetic Investigation on C−H Bond Reductive Coupling in Cluster 2 and Release of the 6-Me-2,2′-bpy Ligand. Wishing to probe the intermediacy of the cluster 1,1-$Os_3(CO)_{10}$(6-Me-2,2′-bpy), the anticipated cluster species from the reaction of **1** and 6-Me-2,2′-bpy, and its role in the C−H bond activation that accompanies the formation of the kinetic hydride **2**, we performed a mechanistic study on the thermolysis of **2** in the presence of trapping ligands. Here the successful trapping of the formal product of C−H bond reductive coupling, the unsaturated cluster 1,1-$Os_3(CO)_9$(6-Me-2,2′-bpy), would be expected to afford 1,1-$Os_3(CO)_9$L(6-Me-2,2′-bpy) (where L = trapping ligand), which could then provide insight into the C−H bond oxidative coupling, as dictated by the principle of microscopic reversibility.

Our initial studies on the reactivity of **2** with various $2e^-$ donors were investigated by UV−vis spectroscopy over the temperature range 318−338 K, with the progress of each reaction monitored by following the decrease in the absorbance of the 540 nm band belonging to **2**. Figure 3 shows UV−vis spectral changes for the reaction of **2** in toluene at 333 K in the presence of a 10-fold excess of $P(OMe)_3$, while the absorbance versus time plot depicted in the inset reveals excellent agreement between the least-squares fit for the first-order decay of **2** and the absorbance data. The first-order rate constants for these reactions are summarized in Table 3; the collective insensitivity of the rate constant to different ligands and variation in the

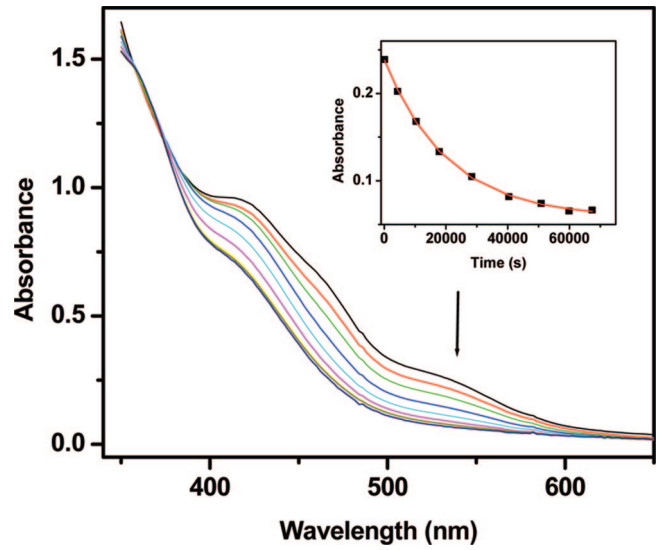

Figure 3. UV−vis spectral changes for cluster **2** in the presence of $P(OMe)_3$ (10 equiv) recorded at 333 K in toluene, with the inset showing the absorbance versus time curve for the experimental data of the first-order rate constant k.

concentration of added ligand supports a rate-limiting step that involves only cluster **2**. Although not examined in detail, the effect of solvent on the reaction of **2** with added ligand is assumed to be negligible, at least between toluene and CH_2Cl_2 given the similarity of the rate constants in these solvents. The zero-order dependence on ligand and the Eyring activation parameters [$\Delta H^{\ddagger} = 21.7(4)$ kcal/mol; $\Delta S^{\ddagger} = -13(1)$ eu] clearly negate rate-limiting steps based on a dissociative ligand loss and an associative ligand attack on cluster **2**.

The fate of **2** upon reaction with excess CO and $P(OMe)_3$ was ascertained by a combination of IR and ^{1}H NMR spectroscopies and independent syntheses of the suspected end products. Heating **2** in CH_2Cl_2 or toluene solvent at 333 K under 6.8 atm CO led to the formation of parent cluster $Os_3(CO)_{12}$, as determined by IR monitoring of the reaction solution.[26] Parallel preparative experiments also produced $Os_3(CO)_{12}$ in near quantitative yields (>95%) after chromatographic purification. An analogous reaction between **2** and CO (6.8 atm) was studied by ^{1}H NMR spectroscopy in $CDCl_3$ in the presence of the internal standard ferrocene. Here samples that were analyzed as a function of time verified the release of free 6-Me-2,2′-bpy with a mass balance of 97%. The reaction of **2** with $P(OMe)_3$ was also examined and spectroscopic evidence (IR and ^{1}H and ^{31}P NMR) was obtained for the liberation of 6-Me-2,2′-bpy and formation of the cluster 1,2,3-$Os_3(CO)_9[P(OMe)_3]_3$, whose synthesis and spectral properties have been reported earlier by Pomeroy.[27] Samples of 1,2,3-$Os_3(CO)_9[P(OMe)_3]_3$ that were isolated from preparative reactions of **2** with $P(OMe)_3$ matched independently prepared samples of the Pomeroy cluster. The outcome of the CO and $P(OMe)_3$ trapping studies described here is illustrated by eq 6.[28,29]

Kinetic studies for the reaction of **2** with excess $P(OCD_3)_3$ and PPh_3 were also investigated by ^{1}H NMR spectroscopy. Since the concentration requirements for **2** in NMR kinetics are greater by a factor of 10^2 compared to the UV−vis studies, we employed CD_2Cl_2 rather than toluene-d_8 as the NMR solvent

(26) These carbonylation reactions were conducted at constant CO pressure using a Fisher-Porter tube equipped with a tip tube for periodic sampling.

(27) Alex, R. F.; Pomeroy, R. K. *Organometallics* **1987**, *6*, 2437.

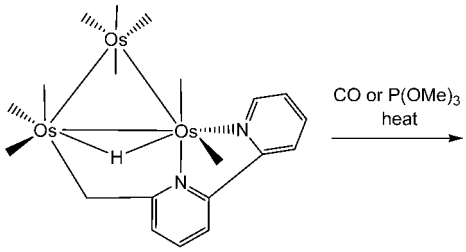

$HOs_3(CO)_9(\mu\text{-}CH_2N_2C_{10}H_7)$ (**2**)

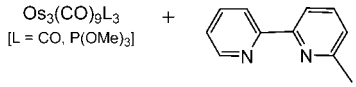

Eq 6

6-Me-2,2'-bpy

due to the higher solubility of cluster **2** in the former solvent. Our choice of $P(OCD_3)_3$ as a trapping ligand was necessary in order to eliminate the intense methoxy resonance from $P(OMe)_3$ that overlapped and saturated the region containing the bipyridyl methylene and methyl groups. A sealed NMR tube containing **2** and $P(OCD_3)_3$ was heated at 333 K, and the extent of the reaction was analyzed by measuring the intensity changes of the methylene hydrogens at δ 2.87. The reaction was kinetically well-behaved, and a plot of ln[**2**] versus time afforded the rate constant quoted in Table 3 (entry 18). A comparable rate constant was also obtained for the consumption of **2** when the high-field doublet of the 6′ hydrogen at δ 9.27 was employed as the probe resonance and its intensity monitored relative to the ferrocene reference. The release of free 6-Me-2,2′-bpy in 97% yield was verified by ^{1}H NMR spectroscopy. The reaction between **2** and PPh_3 proceeded similarly (entry 19, Table 3) with the liberation of 6-Me-2,2′-bpy, whose presence was ascertained by the growth of the methyl singlet at δ 2.48. Under no circumstances did we observe the buildup of any species that could be reconciled with the formation of $Os_3(CO)_9L$(6-Me-2,2′-bpy), the ligand-trapped product from the unsaturated cluster $Os_3(CO)_9$(6-Me-2,2′-bpy).

The role played by reductive coupling of the hydride and cyclometalated alkyl moiety in the rate-limiting step in the conversion of **2** to $Os_3(CO)_{12}$ and 1,2,3-$Os_3(CO)_9[P(OMe)_3]_3$ was next explored through the synthesis of the isotopically labeled heterocycle 6-Me-d_3-2,2′-bpy. Treatment of 2,2′-bpy with Me-d_3-Li (>99% deuterium) in Et_2O, followed by oxidative workup of the dihydro adduct 6-methyl-d_3-1,6-dihydro-2,2′-bipyridine, gave the d_3-isotopomer 6-Me-d_3-2,2′-bpy as a colorless oil. The ^{1}H NMR spectrum of 6-Me-d_3-2,2′-bpy confirmed the absence of the high-field methyl resonance and the presence of seven bipyridyl hydrogens, whose integrated intensities and chemical shifts matched those of the d_0 isotopomer. The extent of deuteration was further corroborated by GC-MS and the observation of a strong parent ion having a *m*/*z* value of 173.0 (cf. the *m*/*z* value of 170.0 found for the 6-Me-d_0-2,2′-bpy ligand recorded under identical conditions).

(28) The kinetics for the reaction of cluster 2 and PPh_3 (10 equiv) were also monitored by ^{1}H NMR spectroscopy (see entry 19, Table 3), and while the experimentally measured rate constant matched the other rate data reported in Table 3, the tris-substituted cluster, if formed, was not the major osmium-containing material. Tentatively, we believe that two PPh_3 ligands add to the cluster, followed by an *ortho* metalation of one of the phosphine ligands. This premise is based on the observation of two, overlapping high-field doublets at ca. δ−15.80 in the ^{1}H NMR spectrum. See ref 29 for related triosmium clusters containing *ortho*-metalated PPh_3 ligands from the thermolysis of $Os_3(CO)_{12}$ and PPh_3.

(29) (a) Gainsford, G. J.; Guss, J. M.; Ireland, P. R.; Mason, R.; Bradford, C. W.; Nyholm, R. S. *J. Organomet. Chem.* **1972**, *40*, C70. (b) Bradford, C. W.; Nyholm, R. S. *J. Chem. Soc., Dalton Trans.* **1973**, 529.

Table 3. Experimental Rate Constants for the Thermolysis of Cluster 2 in the Presence of Ligand-Trapping Agents[a]

entry	temp (K)	solvent	ligand trap	10^5k (s^{-1})
1	318	toluene	CO, 1 atm	1.05 ± 0.02
2	323	toluene	CO, 1 atm	1.72 ± 0.01
3	323	toluene	PPh_3, 10 equiv	1.49 ± 0.04
4	323	CH_2Cl_2	PPh_3, 10 equiv	2.70 ± 0.09
5	323	toluene	PPh_3, 25 equiv	1.74 ± 0.01
6	323	toluene	PPh_3, 50 equiv	2.31 ± 0.04
7	328	toluene	CO, 1 atm	3.16 ± 0.03
8	333	toluene	CO, 1 atm	5.02 ± 0.05
9	333	toluene	CO, 3.4 atm	4.3 ± 0.2[b]
10	333	toluene	CO, 6.8 atm	4.8 ± 0.1[b]
11	333	toluene	CO, 34 atm	5.8 ± 0.4[b]
12	333	toluene	PPh_3, 10 equiv	5.90 ± 0.03
13	333	toluene	PCy_3, 10 equiv	4.65 ± 0.02
14	333	toluene	$P(OMe)_3$, 10 equiv	4.86 ± 0.04
15	333	CH_2Cl_2	$P(OMe)_3$, 10 equiv	5.72 ± 0.03
16	333	CH_2Cl_2	$P(OCD_3)_3$,10 equiv	6.63 ± 0.05
17	333	CH_2Cl_2	PMe_3, 10 equiv	8.0 ± 0.1
18	333	CD_2Cl_2	$P(OCD_3)_3$, 10 equiv	10.0 ± 0.4[c]
19	333	CD_2Cl_2	PPh_3, 10 equiv	6.6 ± 0.2[c]
20	338	toluene	CO, 1 atm	8.36 ± 0.04

[a] The UV−vis kinetic data were collected in the specified solvent using a ca. 10^{-4} M solution of cluster **2** by following the decrease in the absorbance of the 540 nm band. [b] Reaction carried out in an autoclave at constant CO pressure using a ca. 10^{-4} M solution of cluster **2**. [c] Rate constant determined by ^{1}H NMR using a ca. 10^{-2} M solution of **2** in CD_2Cl_2.

Table 4. Experimental Rate Constants for the Thermolysis of Cluster 2-d_3 in the Presence of Ligand-Trapping Agents[a]

entry	temp (K)	solvent	ligand trap	10^5k (s^{-1})
1	323	toluene	CO, 1 atm	1.07 ± 0.01
2	323	toluene	PPh_3, 10 equiv	1.12 ± 0.01
3	323	toluene	PPh_3, 25 equiv	1.18 ± 0.03
4	333	toluene	CO, 1 atm	2.55 ± 0.01
5	333	toluene	CO, 6.8 atm	2.33 ± 0.09[b]
6	333	CH_2Cl_2	$P(OMe)_3$, 10 equiv	2.50 ± 0.02
7	333	CH_2Cl_2	$P(OCD_3)_3$, 10 equiv	3.24 ± 0.03
8	333	CD_2Cl_2	$P(OCD_3)_3$, 10 equiv	3.8 ± 0.2[c]

[a] The UV−vis kinetic data were collected in the specified solvent using a ca. 10^{-4} M solution of cluster **2**-d_3 by following the decrease in the absorbance of the 540 nm band. [b] Reaction carried out in an autoclave at constant CO pressure using a ca. 10^{-4} M solution of cluster **2**-d_3. [c] Rate constant determined by ^{1}H NMR using a ca. 10^{-2} M solution of **2**-d_3 in CD_2Cl_2.

The desired cluster $DOs_3(CO)_9(\mu_2\text{-}CD_2N_2C_{10}H_7)$ (**2**-d_3) and its isomeric isotopomer $HOs_3(CO)_9(\mu_2\text{-}N_2C_{11}H_6D_3)$ (**3**-d_3) were prepared, isolated, and fully characterized in solution by IR and NMR spectroscopies and by FAB mass spectrometry, as outlined in the Experimental Section. Kinetic studies for the reaction of **2**-d_3 with CO, PPh_3, and $P(OMe)_3$-$d_{0,3}$ were performed, and the isotope effect on the reaction was evaluated at 323 and 333 K. UV−vis analysis, as previously described, provided the rate constants quoted in Table 4. A parallel ^{1}H NMR experiment using **2**-d_3 was carried out in CD_2Cl_2 at 333 K under pseudo-first-order conditions with $P(OCD_3)_3$. The decay of the downfield 6′ hydrogen at δ 9.27 allowed the rate of the reaction to be easily followed, and the rate constant (entry 8, Table 4) was subsequently determined by graphical analysis. Using an average value for the rate constants reported in Tables 3 and 4 leads to a kinetic isotope effect (KIE) of 1.78 (323 K) and 2.09 (333 K).

Collectively taken, the kinetic data and the normal KIE for the reaction of **2** with donor ligands strongly suggest a rate-limiting step involving the reductive coupling of the hydride ligand in **2** and the cyclometalated alkyl moiety. Scheme 1 outlines the likely sequence of events using CO as the trapping ligand. It is proposed that C−H bond formation gives rise to a

Scheme 1

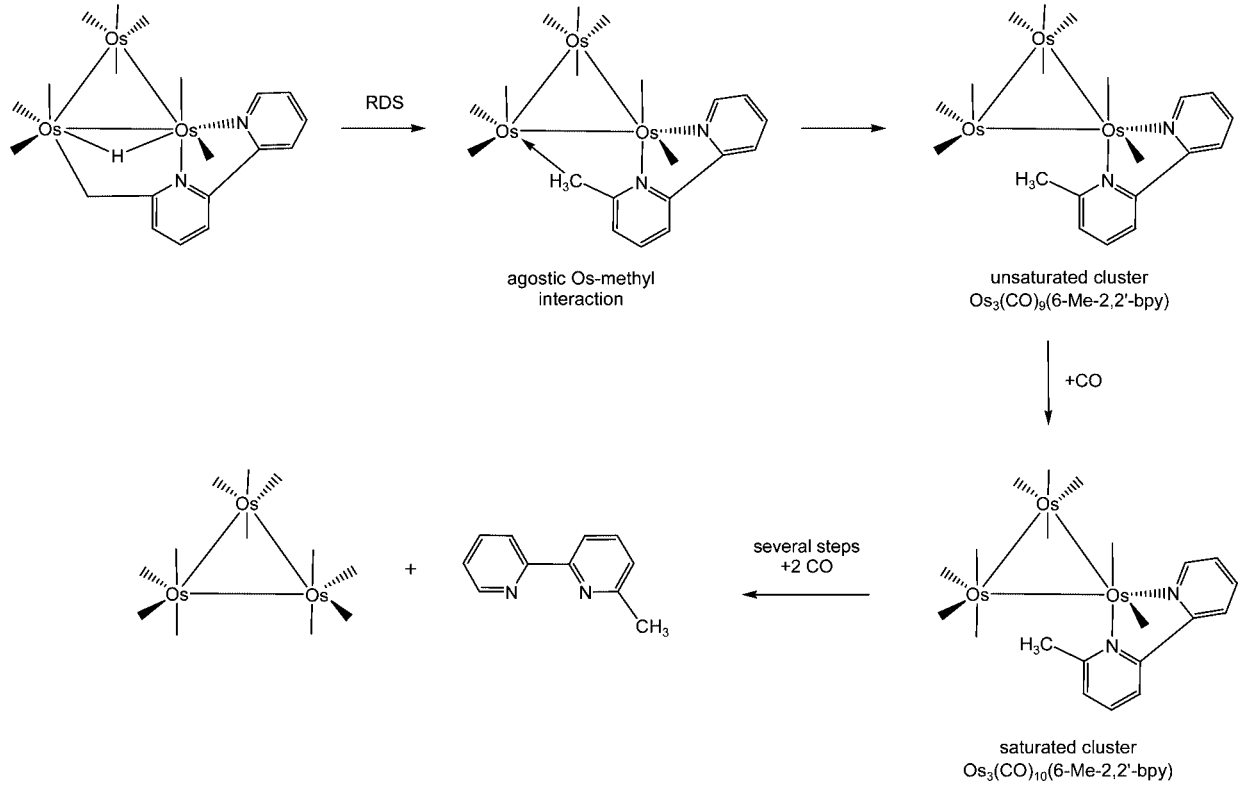

transient agostic complex where the methyl group functions as a weakly bound donor ligand.[30,31] Dissociation of the methyl group from the cluster follows the rate-limiting step and generates the unsaturated cluster $Os_3(CO)_9$(6-Me-2,2′-bpy), which rapidly captures CO to afford the saturated decacarbonyl cluster $Os_3(CO)_{10}$(6-Me-2,2′-bpy).[32] The steric congestion in the latter cluster provides the driving force for the rapid dissociation of the 6-Me-2,2′-bpy ligand and uptake of two additional CO groups.[2a,33]

III. Ligand Substitution Kinetics in Cluster 3 and Formation of $HOs_3(CO)_9[P(OMe)_3](\mu_2\text{-}N_2C_{11}H_9)$ Due to Partial Dissociation of the Chelating Bipyridyl Ligand. The reactivity of cluster **3** with CO and $P(OMe)_3$ was investigated in order to assess the ease of reductive coupling of the hydride and the *ortho*-metalated pyridyl carbon. Preliminary experiments quickly confirmed that the reaction between **3** and CO and $P(OMe)_3$ exhibited disparate rates, indicative of a ligand-dependent process.[34] The ligand dependence was unequivocally established by using $P(OMe)_3$ since the ligand concentrations could be more easily adjusted and measured with greater accuracy than CO. The reactions were explored by UV−vis spectroscopy over the temperature range 333−356 K in toluene and CH_2Cl_2 solvents, with reactions conducted in the former solvent being faster by a factor of ca. 2×. The progress of each reaction was followed by monitoring the decrease in the 540 nm absorbance band for **3**, as illustrated in Figure 4 for the absorbance changes for **3** in the presence of $P(OMe)_3$ (26 equiv) at 356 K in toluene. The pseudo-first-order rate constants quoted in Table 5 were obtained from nonlinear regression analysis of the absorbance versus time curve, as exemplified by the inset accompanying Figure 4. Plots of the pseudo-first-order rate constants (k_{obsd}) as a function of $P(OMe)_3$ were found to be linear with intercepts of zero within experimental error, as illustrated by Figure 5. The slopes of these plots afforded the second rate constants shown in Table 6, which in turn yielded the activations parameters $\Delta H^{\ddagger} = 13.0(3)$ kcal/mol and $\Delta S^{\ddagger} = -30(1)$ eu, which strongly support an associative mechanism involving the attack of a ligand on cluster **3** in the rate-limiting step.

(30) The proposed rate-limiting step involving cluster **2** and the corresponding cluster containing an agostically bound methyl group (i.e., a σ-bound methyl moiety), prior to the formal generation of a vacant coordination site through dissociation of the methyl group, is consistent with the current body of knowledge for alkane activation at mononuclear compounds (see ref 31). An alternative rate-limiting step proceeding by a direct reductive coupling of the C−H bond and formation of an unsaturated cluster in a single step cannot be eliminated from consideration on the basis of the data at hand. Differentiation of these two scenarios is thwarted by our inability to isolate the carbonylation product $Os_3(CO)_{10}$(6-Me-2,2′-bpy) in the reductive coupling step and in the initial reaction of 6-Me-2,2′-bpy with cluster **1**. Here the preparation of the isotopically substituted derivatives $Os_3(CO)_{10}$(6-Me-$d_{1,2}$-2,2′-bpy) would, in theory, help clarify the details associated with the activation of the methyl group in the reductive coupling and oxidative coupling steps.

(31) For reports and reviews on C−H bond activation in alkanes by mononuclear compounds and the isotope techniques employed in the mechanistic study of these reactions, see:(a) Buchanan, J. M.; Stryker, J. M.; Bergman, R. G. *J. Am. Chem. Soc.* **1986**, *108*, 1537. (b) Parkin, G.; Bercaw, J. *Organometallics* **1989**, *8*, 1172. (c) Bullock, R. M.; Headford, C. E. L.; Hennessy, K. M.; Kegley, S. E.; Norton, J. R. *J. Am. Chem. Soc.* **1989**, *111*, 3897. (d) Jones, W. D. *Acc. Chem. Res.* **2003**, *36*, 140. (e) Churchill, D. G.; Janak, K. E.; Wittenberg, J. S.; Parkin, G. *J. Am. Chem. Soc.* **2003**, *125*, 1403. (f) Lersch, M.; Tilset, M. *Chem. Rev.* **2005**, *105*, 2471. (g) Northcutt, T. O.; Wick, D. D.; Vetter, A. J.; Jones, W. D. *J. Am. Chem. Soc.* **2001**, *123*, 7257.

(32) In the absence of suitable trapping ligands the thermodynamically more stable hydride-bridged cluster **3** and the dihydride-bridged cluster **4** are formed. The latter product is presumed to originate from cluster **2** through a slower CO loss pathway at elevated temperatures.

(33) Whether the displacement of the 6-Me-2,2′-bpy ligand from the saturated $Os_3(CO)_{10}$(6-Me-2,2′-bpy) cluster by CO occurs by a dissociative or associative process cannot be determined on the basis of the available data.

(34) Using the published solubility data for CO in toluene, we estimate the molar ratio of cluster **3** to CO (1 atm) at 333 K as 1:75. See: Basickos, L.; Bunn, A. G.; Wayland, B. B. *Can. J. Chem.* **2001**, *79*, 854.

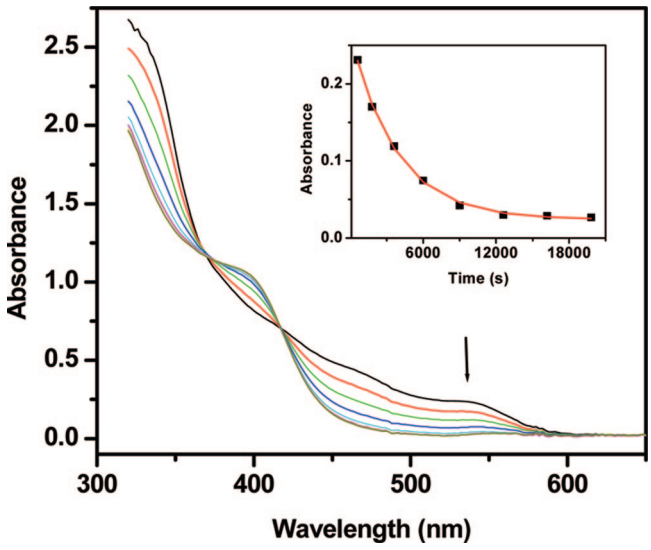

Figure 4. UV−vis spectral changes for cluster **3** and $P(OMe)_3$ (26 equiv) recorded at 356 K in toluene, with the inset showing the absorbance versus time curve for the experimental data of the psuedo-first-order rate constant k_{obsd}.

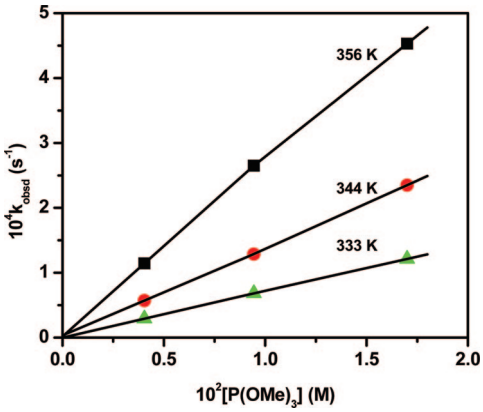

Figure 5. Plots of k_{obsd} versus the concentration of $P(OMe)_3$ in toluene solution as a function of temperature for the reaction of cluster **3** with ligand.

The kinetics for the reaction between **3** and $P(OCD_3)_3$ (11 equiv) were also studied by ^{1}H NMR at 333 K. Monitoring the intensity changes of the methyl singlet in **3** at δ 2.80 yielded the pseudo-first-order constant of $18.8(1) \times 10^{-5}$ s^{-1} that is quoted in Table 5 (entry 6). The diminution of the methyl resonance, as well as the hydride ligand at δ −21.48 in **3**, was accompanied by the growth of two new bipyridyl methyl singlets at δ 2.54 (30%) and 2.43 (70%) and a pair of high-field hydrides at δ −14.62 (30%) and −14.80 (70%). New aromatic resonances at δ 7.55, 7.18−6.90, and 6.50 having an integral ratio of 1:4:1, respectively, replaced the bipyridyl hydrogens of **3** as the reaction proceeded to completion. A total of six aromatic hydrogens in the new product indicates that the bipyridyl moiety is bound to the cluster polyhedron by an *ortho*-metalated bipyridyl moiety. The nature of the product formed from the reaction of **3** with $P(OMe)_3$ was subsequently established by spectroscopic methods and mass spectrometry. The single product isolated from a preparative reaction between **3** and $P(OMe)_3$ exhibited two ^{31}P resonances at δ 114.08 (30%) and 116.25 (70%), confirming the presence of a $P(OMe)_3$ ligand in the products, whose relative ratios parallel the methyl and hydride ratios found in the kinetics experiment. That two $P(OMe)_3$-containing clusters were present in the product mixture

Table 5. Experimental Rate Constants for the Thermolysis of Cluster 3 in the Presence of Ligand-Trapping Agents[a]

entry	temp (K)	solvent	ligand trap	10^5k_{obsd} (s^{-1})
1	333	toluene	CO, 1 atm	1.22 ± 0.04
2	333	toluene	$P(OMe)_3$, 11 equiv	2.92 ± 0.01
3	333	CH_2Cl_2	$P(OMe)_3$, 11 equiv	1.51 ± 0.01
4	333	toluene	$P(OMe)_3$, 26 equiv	6.83 ± 0.02
5	333	CH_2Cl_2	$P(OMe)_3$, 26 equiv	2.95 ± 0.01
6	333	CD_2Cl_2	$P(OCD_3)_3$, 11 equiv	18.8 ± 0.1[b]
7	333	toluene	$P(OMe)_3$, 53 equiv	12.13 ± 0.03
8	338	toluene	CO, 1 atm	1.58 ± 0.01
9	344	toluene	CO, 1 atm	2.50 ± 0.01
10	344	toluene	$P(OMe)_3$, 11 equiv	5.71 ± 0.04
11	344	toluene	$P(OMe)_3$, 26 equiv	12.88 ± 0.08
12	344	toluene	$P(OMe)_3$, 53 equiv	23.5 ± 0.2
13	351	toluene	CO, 1 atm	4.29 ± 0.02
14	356	toluene	CO, 1 atm	6.22 ± 0.04
15	356	toluene	$P(OMe)_3$, 11 equiv	11.44 ± 0.05
16	356	toluene	$P(OMe)_3$, 26 equiv	26.5 ± 0.7
17	356	toluene	$P(OMe)_3$, 53 equiv	45.3 ± 0.6

[a] The UV−vis kinetic data were collected in the specified solvent using a ca. 10^{-4} M solution of cluster **3** by following the decrease in the absorbance of the 540 nm band. [b] Rate constant determined by ^{1}H NMR using a ca. 10^{-2} M solution of **3** in CD_2Cl_2.

Table 6. Ligand-Dependent Rate Constants for the Thermolysis of Cluster 3 with $P(OMe)_3$

temp (K)	10^3k_2 (M^{-1} s^{-1})
333	7.08 ± 0.08
344	13.70 ± 0.02
356	26.0 ± 0.9

was also reflected in the ^{1}H NMR spectrum, where two methoxy doublets were observed δ 3.59 (30%) and 3.39 (70%). The other ^{1}H resonances nicely matched those data recorded in the kinetics experiment. The ESI mass spectrum revealed a parent ion at *m/e* 1118.57 that is consistent with a cluster having the composition $HOs_3(CO)_9[P(OMe)_3](\mu_2\text{-}N_2C_{11}H_9)$. Taken collectively, the kinetics, NMR, and mass spectral data support the attack of a $P(OMe)_3$ ligand on cluster **3** and release of the methyl-substituted pyridine ring from the cluster to give the phosphite-substituted cluster $HOs_3(CO)_9[P(OMe)_3](\mu_2\text{-}N_2C_{11}H_9)$ (**5**), which exists as a pair of isomers having a pendant or dangling pyridyl group. This reaction is depicted in eq 7.

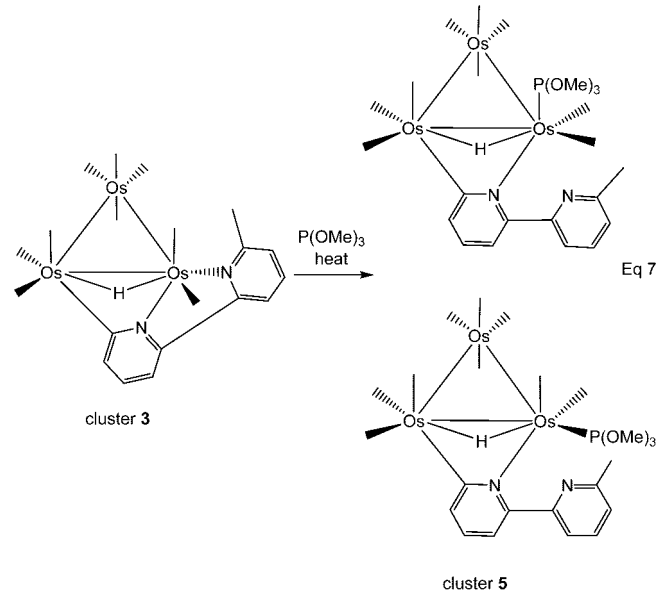

Eq 7

Our formulation for cluster **5** is strengthened by an earlier report from Lewis and co-workers, where the reaction of the

pyridyl-metalated cluster $HOs_3(CO)_{10}(\mu_2\text{-}NC_5H_4)$ with $P(OMe)_3$ was found to furnish $HOs_3(CO)_9[P(OMe)_3](\mu_2\text{-}NC_5H_4)$, as depicted in eq 8.[35,36] The close match between the IR and NMR data for $HOs_3(CO)_9[P(OMe)_3](\mu_2\text{-}NC_5H_4)$ and cluster **5** supports the existence of structurally similar pyridyl-bridged triosmium clusters.

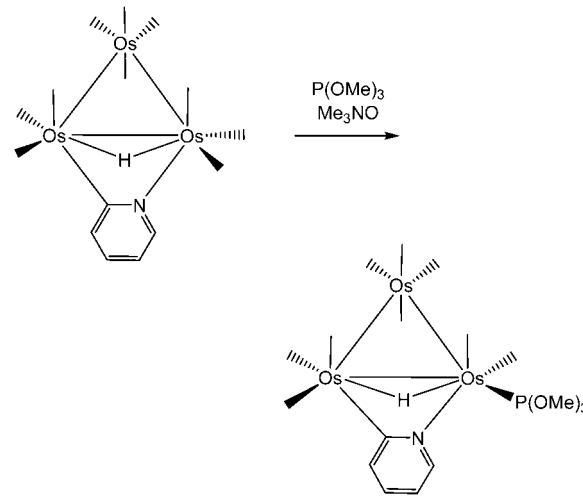

Eq 8

Conclusions

The reaction between the activated cluster $Os_3(CO)_{10}(MeCN)_2$ and the ligand 6-Me-2,2′-bpy proceeds readily at room temperature to give the isomeric hydride-bridged clusters $HOs_3(CO)_9(\mu_2\text{-}CH_2N_2C_{10}H_7)$ (**2**) and $HOs_3(CO)_9(\mu_2\text{-}N_2C_{11}H_9)$ (**3**). The kinetically formed cluster **2** transforms into cluster **3** upon heating in an effort to relieve the steric congestion that accompanies the chelation of the α-diimine ligand and cyclometalation of the methyl group. The driving force for the isomerization of **2** → **3** is currently under computational investigation, and these data will provide the basis of a future report. The kinetics for C−H bond reductive coupling in **2** have been studied and data presented on the lability of the putative cluster 1,1-$Os_3(CO)_9$L(6-Me-2,2′-bpy) [where L = CO, $P(OMe)_3$], which readily releases the α-diimine ligand in the presence of additional trapping ligand. The demonstration of cluster-mediated activation of the α-methyl substituent in 6-Me-2,2′-bpy, followed by release of the α-diimine ligand upon capture of external trapping ligands by the cluster, provides the basis for a potential synthetic protocol for side-chain modification of heterocyclic ligands. The generality of the kinetic and thermodynamic activation of different alkyl and aryl moieties in α-substituted α-diimine ligands is currently under investigation by our groups.

Acknowledgment. Financial support from the NSF (C.J.C.) and Robert A. Welch Foundation (Grant B-1093, M.G.R.) is greatly appreciated. The NSF-MRI program grant CHE-0320848 is gratefully acknowledged for support of the X-ray diffraction facilities at San Diego State University.

OM800020X

(35) Ditzel, E. J.; Johnson, B. F. G.; Lewis, J. *J. Chem. Soc., Dalton Trans.* **1987**, 1293.

(36) The substitution site for the ancillary $P(OMe)_3$ ligand in $HOs_3(CO)_9[P(OMe)_3](\mu^2\text{-}NC_5H_4)$ has been assigned by using NMR spectroscopy, making use of the $^2J_{P-H}$ value and spectral comparisons to related clusters. Here the specific locus of the phosphite ligand may be confidently assigned to a site on the cluster that is *cis* to the bridging hydride ligand, with eq 8 showing one of four possible stereoisomeric products.